Groundwater for Sustainable Development 9 (2019) 100279

Contents lists available at ScienceDirect

Groundwater for Sustainable Development

journal homepage: http://www.elsevier.com/locate/gsd

Research paper

Simulation of groundwater level using MODFLOW, extreme learning machine and Wavelet-Extreme Learning Machine models

Maryam Malekzadeh [a], Saeid Kardar [b,*], Saeid Shabanlou [c]

[a] Department of Environment, Tehran North Branch, Islamic Azad University, Tehran, Iran
[b] Department of Architecture, Science and Research Branch, Islamic Azad University, Tehran, Iran
[c] Department of Water Engineering, Kermanshah Branch, Islamic Azad University, Kermanshah, Iran

ARTICLE INFO

Keywords:
Groundwater level
MODFLOW
Extreme learning machine
Wavelet
Uncertainty analysis

ABSTRACT

Due to the need to forecast changes in groundwater systems and environment, groundwater modeling has been emerged. In this study, the groundwater level of the Kabodarahang aquifer located in Iran, Hamadan Province is simulated by means of three models: MODFLOW, Extreme Learning Machine (ELM) and Wavelet-Extreme Learning Machine (WA-ELM). At the beginning, the groundwater level simulation is carried out by MODFLOW with reasonable accuracy so that the correlation coefficient (R^2) and the scatter index (*SI*) are calculated 0.917 and 0.0004, respectively. After that, through different input combinations as well as the stepwise selection, 10 different models are developed as different lags for the ELM and WA-ELM models. Based on the numerical results yielded by all three models, WA-ELM is introduced as the superior model in simulating the groundwater level. For instance, the correlation coefficient (R^2) and the Nash-Sutcliffe efficiency coefficient (*NSC*) are computed 0.959 and 0.915, respectively. According to the uncertainty analysis, it is proved that the superior model has an underestimated performance. Furthermore, the by-products of the model such as weights and biases are then utilized to develop an explicit method for estimating the groundwater level. The developed model can be easily employed by an engineer with sufficient knowledge of matrix operation without prior information about the extreme learning machine. It is as accurate as the developed WA-ELM hybrid model and more precise than ELM and MODFLOW.

1. Introduction

Groundwater is an important natural resource widely used for meeting domestic, industrial and agricultural requirements (Bashi-Azghadi et al., 2010). According to the Koppen climate classification, Iran is classified into the dessert and dry steppes climate and accessing water has always been one of the most important challenges in the whole country. In Iran, seventy billion cubic meters of water is extracted from groundwater resources for various purposes each year, equivalent to two-thirds of the country water usage which highlights the crucial role of groundwater resources in meeting water demands of the country. Furthermore, in recent years, by increasing population and industrial development on a very rapid pace as well as the modernization of agriculture, groundwater resources are gradually declining.

Groundwater resources are stored below the surface of the earth away from direct observation, so full understanding of their properties takes a long time for carrying out many exploratory studies which are very time consuming and expensive. Groundwater models are appropriate tools for continuous quality-quantity monitoring of aquifers. The simulation of groundwater flow by mathematical models is an indirect approach for solving problems by consuming less cost than direct methods. In fact, the purpose of the development of mathematical models is to simulate natural conditions of water tables by means of a series of mathematical relations. Understanding of groundwater resources is improved through the application of mathematical models capable of simulating the dynamics of an aquifer system (Boyce et al., 2015). Due to the need to solve the flow equations in groundwater, the numerical modeling has been begun in most university research centers and consulting engineers since 30 years ago. Finite difference models are superior in practical hydrological works, because their design and understanding are easier and have less mathematical complexity. Furthermore, several finite difference models with good efficiency have been developed by research organizations such as the US Geological Survey and the US Environmental Protection Agency. One of these

* Corresponding author.
E-mail address: Saeid.Kardar@gmail.com (S. Kardar).

https://doi.org/10.1016/j.gsd.2019.100279
Received 25 July 2019; Received in revised form 30 August 2019; Accepted 7 September 2019
Available online 11 September 2019

models is MODFLOW (3D finite difference model of groundwater flows).

Many researchers used MODFLOW to simulate groundwater levels in various areas (Dong et al., 2012; Lachaal et al., 2012; Ou et al., 2013, 2016; Chen et al., 2017). For instance, Coelho et al. (2017) conducted a study based on the field data belonging to an aquifer in a watershed located in Vicosa, Minas Gerias, Brazil to evaluate numerical hydrological models produced using different boundary conditions, because the field data did not allow a good definition of the most appropriate boundary condition for simulating the observed field properties in the study area. They created three numerical hydrological models in Visual MODFLOW and calibrated them using WinPEST®. GHB (General Head boundary), River and Stream boundary conditions resulted in a calibrated standard Root Mean Square (RMS) were in the range of 7.3%–13.02% showing high correlation coefficients in the range of 94%–97%. The results of their study showed that for all three boundary conditions, the normalized RMS resulted from calibration was similar to that resulted from validation which confirms its validity.

In recent years, soft computing methods have been used to simulate and estimate various phenomena (Liu et al., 2008; Dastorani et al., 2010; Heddam et al., 2012; Ghumman et al., 2018). Ebrahimi and Rajaee (2017) by collecting data from two wells situated in the Qom plain tried to simulate groundwater level. In their study, the influence of a wavelet analysis on training of the Artificial Neural Network (ANN), Multi Linear Regression (MLR) and Support Vector Regression (SVR) methods was evaluated. Then, they compared ANN, MLR and SVR with the wavelet-ANN, wavelet-MLR and wavelet-SVR models in simulating one-month-ahead of groundwater level. They concluded that the decomposition of groundwater level time series into sub-time series noticeably enhances training of the models. They found that for both wells, the Meyer and Daubechies-5 (Db5) mother wavelets obtain more accurate results than other wavelets. Barzegar et al. (2017) simulated the Maraghe-Bonab aquifer in order to evaluate the performance of the Wavelet-Group Method of the Data Handling (WA-GMDH) approach and WA-ELM models as well as combining wavelet based models for modeling groundwater level. They employed 367 monthly groundwater level datasets for training and evaluating the model. Finally, they concluded that wavelet based models improve the performance of Group Method of Data Handling (GMDH) and the ELM model in simulating groundwater level.

An increasing number of studies have specifically examined the application of numerical models and soft computing techniques in simulating groundwater level. Due to simple modeling, easy coding and fast computation in simulating complex yet practical fields of science, ELM has recently gained more attention than other tools. The ELM models are rarely used probably because they do not significantly improve the accuracy compared to empirical formulae and/or few engineers are familiar with the ELM models. To overcome these problems, first we develop an ELM model in conjunction with the db2 mother wavelet transform in order to enhance the accuracy of the model. Exploring the literature demonstrates that no previous studies has been carried out on the groundwater level prediction of the Kabodarahang aquifer located in Iran, Hamadan Province, by utilizing the extreme learning machine (ELM) in conjunction with the wavelet transform (WA-ELM). Different normalization approaches and mother wavelet families in combination with different inputs produced by the "stepwisefit" function in the MATLAB environment are considered to present the optimum model. The result of the proposed hybrid method is compared with ELM as an artificial intelligence based method and MODFLOW as a physically based technique. Moreover, a WA-ELM based model is developed to estimate groundwater level by engineers with basic knowledge of matrix operation without sufficient knowledge of ELM.

2. Study area

The Kabodarahang Plain has an area of 3470 square kilometers located in the north of Hamadan province. This region has a semi-arid to dry and cold climate. The main source of atmospheric precipitation of this region is the Mediterranean, and the main source of air humidity and rainfall is provided by western fronts. The average precipitation of Kabodarahang plain according to the long term statistics (36 years) is estimated 281.5 mm/year. According to the meteorological organization statistics, the average temperature at the station is 11.1 °C. The average minimum and maximum temperatures are recorded 2.9 °C and 34.4 °C, respectively. The warmest and coldest months of the year are recorded July and January with 40 °C and −32 °C, respectively. The average annual evaporation of this region is estimated to be 1820 mm. The employed dataset in this study is related to 25 years monthly samples (301 samples) from August1990 to September2015.The geographic location of the study area is illustrated in Fig. 1.

3. Materials and methods

3.1. MODFLOW-2000

MODFLOW is a computer program that numerically solves the three-dimensional groundwater flow equation for a porous medium by using a finite-difference method (Harbaugh et al., 2000). The three-dimensional movement of groundwater of constant density through porous earth material may be described by a partial-differential equation.

For many data input quantities, MODFLOW-2000 allows definition using parameter values, each of them can be applied to data input for many grid cells (Harbaugh et al., 2000). This model is almost a complete model for numerical modeling of a system flow in saturated environments, because it has many abilities and subprograms to simulate a groundwater table system. As a widely used groundwater flow model, MODFLOW provides a set of packages in order to simulate hydrological stresses, input and output flows to a groundwater system (Dong et al., 2012). According to different properties, these packages can be classified into three categories including point, line and area properties. The well package (WEL) can simulate a specified recharge or discharge point such as a well. The general head boundary package (GHB) the river package (RIV) and the drain package (DRN) provide line properties of input or output flows to a groundwater system. Area properties such as precipitation, plant transpiration and direct evaporation are modeled using the recharge (RCH) and evapotranspiration (ET) packages (Dong et al., 2012).

In order to perform the model in the steady state, after establishing the model geometric characteristics and completing all necessary packages, a period of relatively stable water levels (1996–1997) is chosen for running the model in the steady state. In this case, the daily average of the recharge and discharge parameters as well as the average water table level in the chosen period are prepared and imported to the conceptual model. In the first step, the model manual adjustment of the level and recharge parameters is done in the model and the outputs are compared with the observational levels. After that, the automatic calibration process is conducted. To carry out the auto-calibration approach, the PEST software runs.

In this study, the study area is delineated in MODFLOW-2000 to establish the model of the Kabodarahang plain aquifer. To this end, the geographical area is processed in the GIS environment and the resulted file is imported to the model. Then, by choosing an appropriate mesh the geographical area is divided into cells. By importing the DEM file of the study area, the elevations of the surface, bottom and thickness of the layer are defined. By considering the study objectives, the transient flow regime is selected for simulating the hydraulics of the groundwater flow. According to the modeling time period (10 years), the hydrological stress periods are applied. The hydrodynamic coefficients of the aquifer such as the hydraulic conductivity and storage coefficients are interpolated and calibrated based on the values obtained from the pumping tests. The agricultural and industrial pumping wells and rivers as well as streams within the study area are applied to the model according to the time steps using the WEL and RIV packages, respectively. The recharge

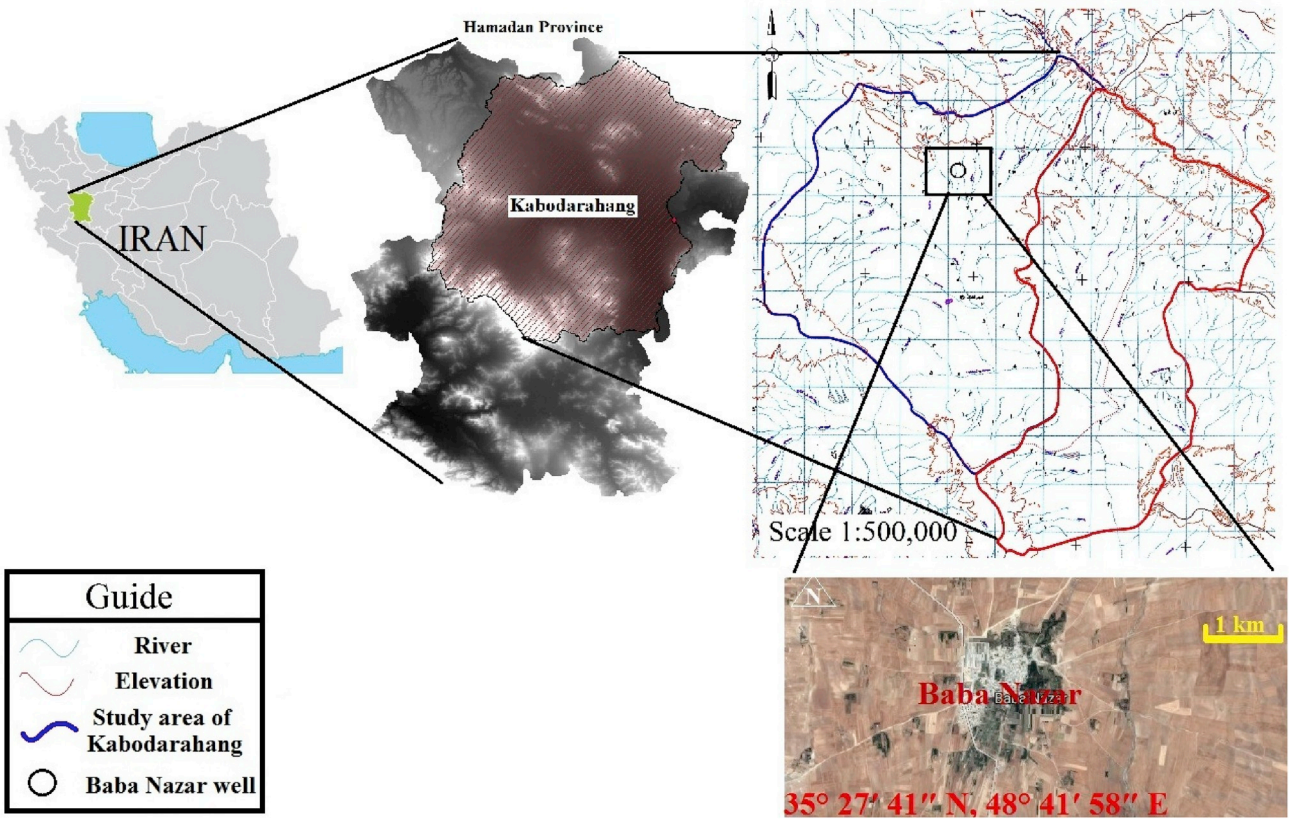

Fig. 1. Geographical location of study area.

coefficient produced by rainfall and runoff as well as return water from agricultural activities in each stress period are estimated using the HEC-HMS model and applied to the MODFLOW groundwater flow model. The recharge coefficient is concluded from the HEC-HMS model and corrected through the trial and error process. After the first run in the transient state, the storage and conductivity parameters as the most effective parameters in the sensitivity analysis are optimized and the model verification performed using the data obtained from 23 wells with acceptable distribution in the study area as the observational data and the difference between calibration heads versus observed heads is obtained in an acceptable range. Finally, in order to obtain the observational values of groundwater level for 120 months, the time series values of the Baba Nazar well located in 35° 27′ 41″ N, 48° 41′ 58″ E are extracted to evaluate fluctuations of groundwater level in this point.

3.2. Methods and model development

First, a review on the Extreme Learning Machine (ELM) as a method based on the powerful computational intelligence which has a good performance in complex non-linear systems and the Discrete Wavelet Transform (DWT) as a suitable time series decomposition method is provided. Then, the model is developed and a combination of two Wavelet and ELM methods called "WA-ELM" is presented.

3.2.1. Extreme learning machine (ELM)

ELM is a training algorithm for the single layer feed-forward- neural network (SLFFNN). The main idea of the algorithm is based on the concept of SLFFNN which with H hidden nodes randomly determines values of input weights and biases of the hidden layer according to continuous probability distribution with probability of 1, so that to be able to train N separate samples.

SLFFNN is provided as a linear system in which hidden node parameters are determined randomly and network output weights are obtained in an analytic way by means of a generalized inverse of the hidden-layer output matrix. ELM has many advantages such better performance, much less modeling time, less modeling error and less weights norm compared to conventional neural networks such as Artificial Neural Networks (ANNs). In conventional neural networks, achieving a good modeling requires adjustment for various parameters such as learning epochs and learning rate, while in ELM, after selecting the type of the activation function, only the number of hidden layer neurons needs to be adjusted. Besides, difficulties such as improper learning rate; local minima and over fitting existing in gradient based

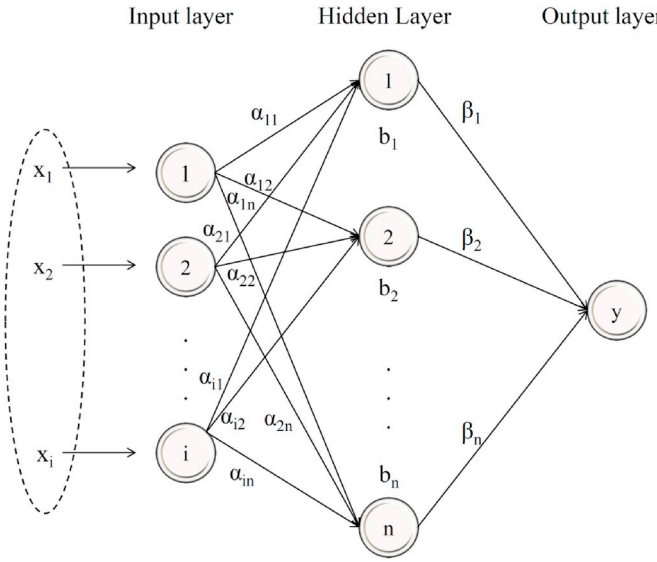

Fig. 2. The structure of ELM.

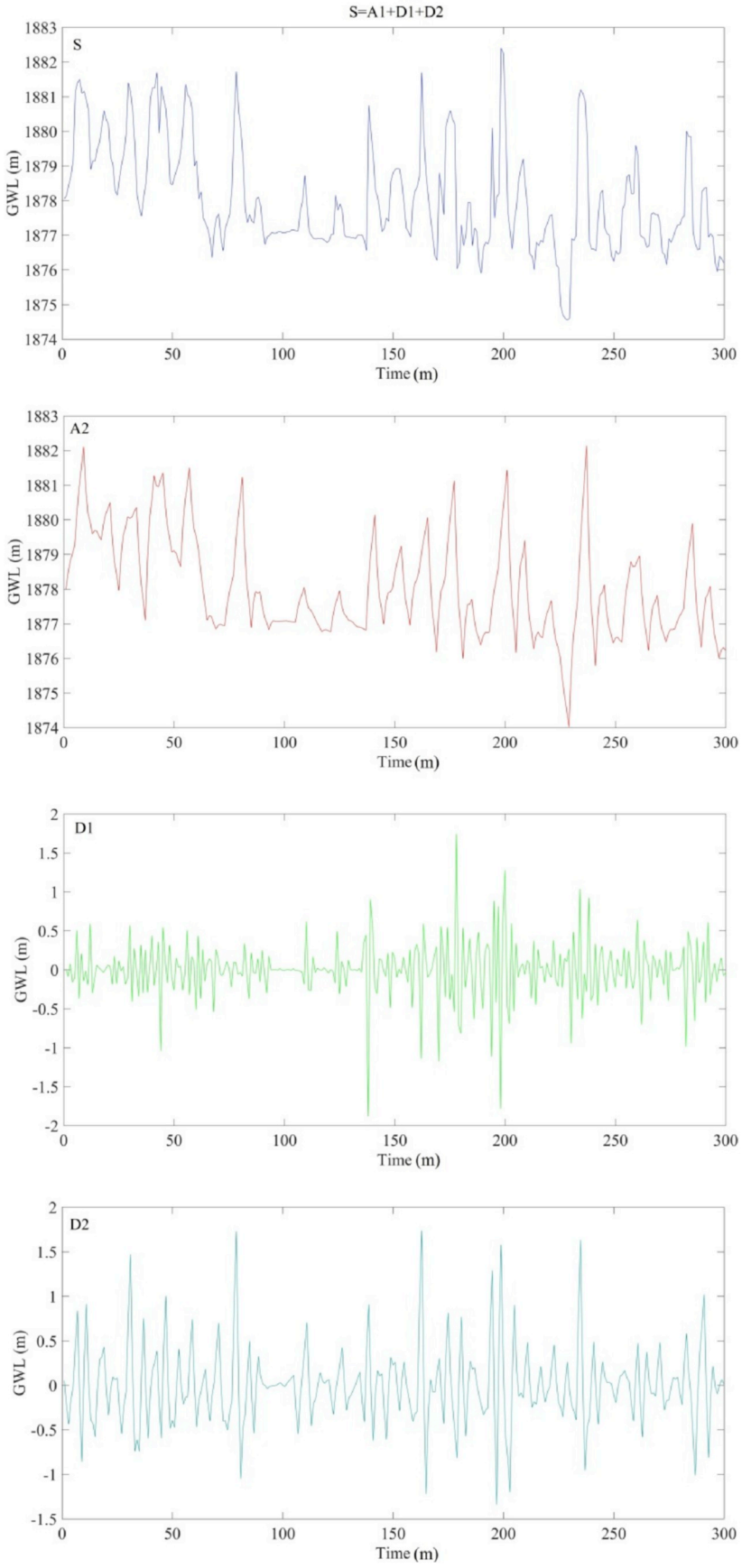

Fig. 3. Two decomposition levels of ground water level (GWL) time series of "Baba Nazar" station performed by Daubechies wavelet.

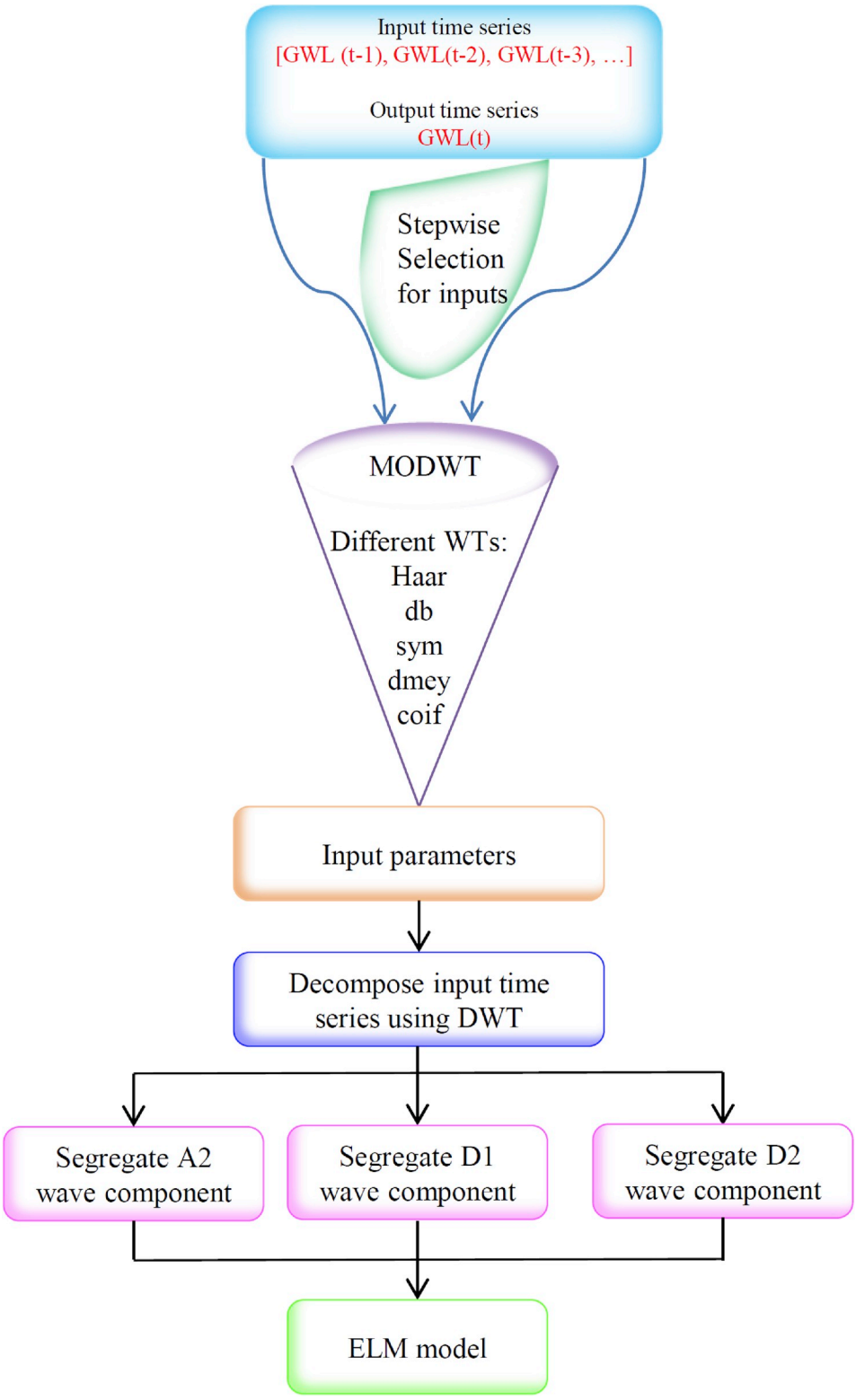

Fig. 4. Flowchart of proposed wavelet-ELM for GWL simulation.

networks are simply addressed by ELM. In addition, training of gradient-based networks is possible only for derivative activation functions, whereas ELM also works well with irreducible functions (Huang et al., 2004). Training of ELM is conducted quickly and its generalization performance is remarkably high. The ability of universal approximation in this method has been proven by Huang et al. (2006); Huang and Chen (2007, 2008).

The structure of the ELM network is depicted in Fig. 2. By considering N optional samples for training the model as (x_i, y_i), where $x_i = (x_{i1}, x_{i2}, ..., x_{in}) \in R^n$ and $y_i = (y_{i1}, y_{i2}, ..., y_{im}) \in R^m$, so that x_i is a $n \times 1$ vector and y_i is a $m \times 1$ vector. By considering the activation function as $g(x)$ and the number of hidden nodes equal to H, the SLFFNN model is rewritten as follows:

$$\sum_{i=1}^{H} \beta_i g_i(x_j) = \sum_{i=1}^{H} \beta_i g_i(a_i.x_j + b_i) \qquad j = 1, 2, ..., N \tag{1}$$

where, $a_i = [a_{i1}, a_{i2}, a_{i3}, \ldots a_{in}]^T$ is the weight vector among hidden and input nodes, $\beta_i = [\beta_1, \beta_2, \beta_3, \ldots, \beta_{im}]^T$ is the weight vector among hidden and output nodes and b_i is the threshold of the ith hidden node. The matrix form of equation (1) is as follows:

$$Y = \sum_{i=1}^{H} \beta_i g_i(x_j) = G\beta \tag{2}$$

where:

$$Y = \begin{bmatrix} y_1^T \\ \vdots \\ y_L^T \end{bmatrix}_{N \times m} \tag{3}$$

$$\beta = \begin{bmatrix} \beta_1^T \\ \vdots \\ \beta_L^T \end{bmatrix}_{H \times m} \tag{4}$$

$$G = \begin{bmatrix} f(a_1.x_1 + b_1) & \cdots & f(a_H.x_1 + b_H) \\ \vdots & \ddots & \vdots \\ f(a_1.x_N + b_1) & \cdots & f(a_H.x_N + b_H) \end{bmatrix}_{N \times H} \tag{5}$$

where, T is the transport operator, β denotes output weights and G is the hidden-layer output matrix. Additionally, the structure of the extreme learning machine is illustrated in Fig. 2.

In order to find least squares responses, the matrix of output weights is expressed as follows:

$$\beta = H^+ Y \tag{6}$$

where, H^+ is the Moore-Penrose generalized inverse (MPGI) of the of hidden-layer output matrix (Y). Moreover, for modeling by ELM, the number of hidden layer neurons and the activation function type should be optimized. In this paper, the trial and error approach is implemented to determine the number of optimized hidden layer neurons. In other words, for a model with a fixed number of inputs, the number of neurons varies from 1 to 25. The results indicate that increasing the number of hidden layer neurons has no noticeable effect on modeling. To this end, the number of hidden layer neurons is considered 19 (equal to the number of optimized hidden layer neurons). Furthermore, for determining the activation function type, five different functions are considered including the sine function (sin), the radial basis function (radbas), the triangular basis function (tribas), the Hardlimit function (hardlim) and the Sigmoid function (sig) which are defined as follows:

$$\text{The sine activation function } (\sin): \; g(a, b, x) = \sin(w \cdot a + b) \tag{7}$$

$$\text{The radial basis activation function } (\text{radbas}): \; g(a, b, x) = \exp\left(-b\|x - c\|^2\right) \tag{8}$$

$$\text{The triangular basis activation function } (\text{tribas}): \; g(a, b, x) = \begin{cases} 1 - |a \cdot x + b|, & a \cdot x + b \geq 0 \\ 0 & otherwise \end{cases} \tag{9}$$

$$\text{The hardlimit activation function } (\text{hardlim}): \; g(a, b, x) = \begin{cases} 1, & if\ a \cdot x + b \geq 0 \\ 0, & otherwise \end{cases} \tag{10}$$

Table 1
Values of statistical indices for different activation functions.

Activation functions	*R*	*VAF*	*RMSE*	*SI*	*MAE*	*MAPE*	*RMSRE*	*BIAS*	*NSC*
Sigmoid	**0.751**	**56.090**	**0.954**	**0.0005**	**0.626**	**0.0003**	**0.0005**	**−0.085**	**0.333**
Sine	0.659	42.210	1.112	0.0006	0.877	0.0005	0.0006	−0.216	0.018
Hardlim	0.034	−2.254	1.549	0.0008	1.276	0.0007	0.0008	−0.543	−6.383
Triangle basis	0.513	15.368	1.321	0.0007	0.990	0.0005	0.0007	−0.074	−0.189
Radial basis	0.651	42.387	1.093	0.0006	0.783	0.0004	0.0006	−0.090	−0.394

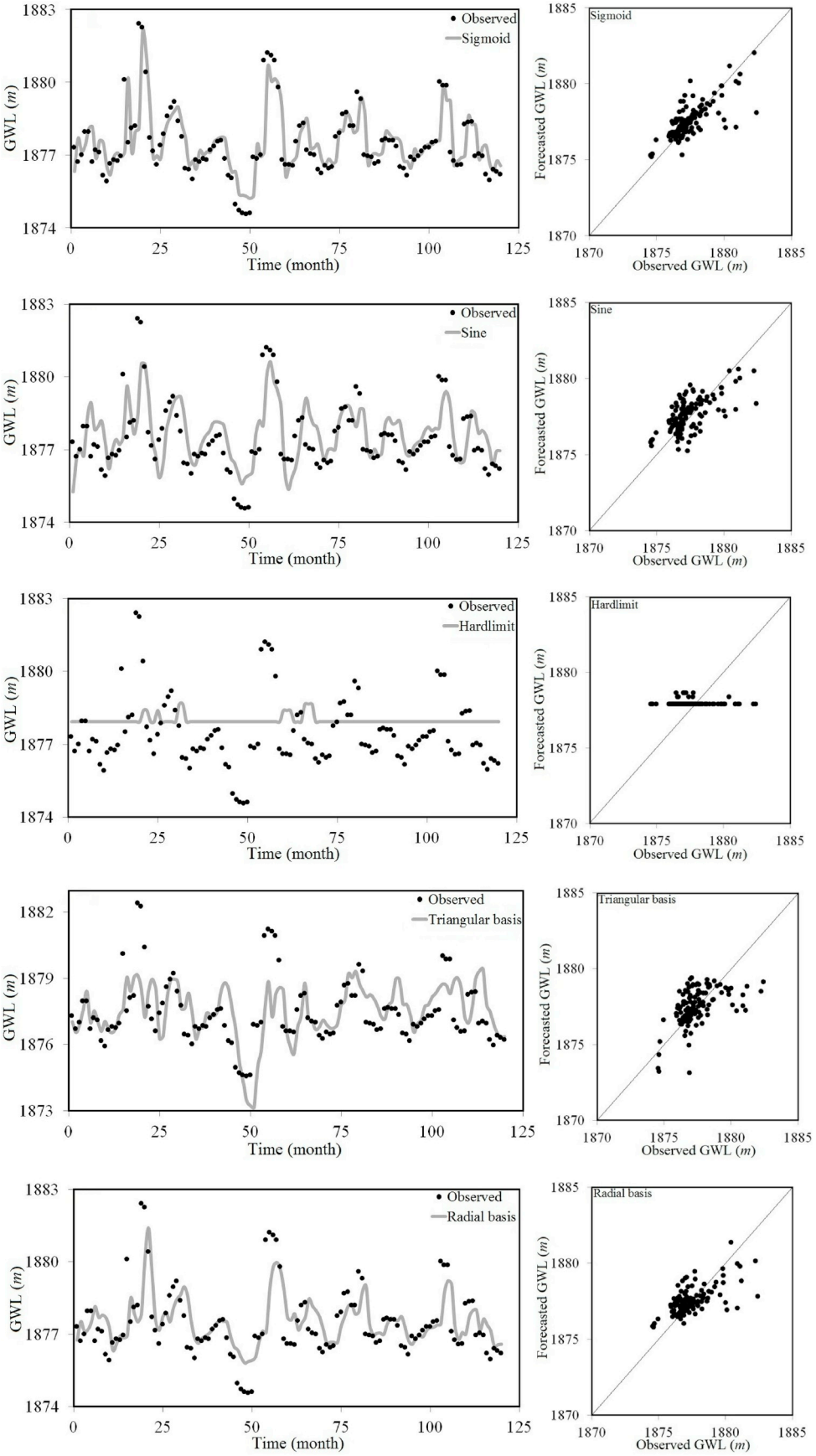

Fig. 5. Simulated groundwater level for different activation functions.

$$\text{The sigmoid activation function } \left(\text{sig}\right): \; g(a,b,x) = \frac{1}{1+\exp(-(a,b,x))} \tag{11}$$

3.2.2. Wavelet transform

Wavelet is a transformation tool utilized for decomposition, compression and de-noising. This method is a time independent spectral analysis decomposing time-series in the frequency-time environment in order to describe the time-scale, processes and their relations (Daubechies, 1990). Similar to the Fourier transform, the Wavelet transform considers time series as a linear combination of multiple base functions. One of the main features of the Wavelet transform is its ability to achieve time, frequency and situation data simultaneously (Misiti et al., 1996). The continuous wavelet transform (CWT) is able to operate in any scale, although calculating the wavelet coefficients in any scale is difficult and requires long computational time and producing a large amount of data. In the discrete wavelet transform (DWT) only one subset of scales and situations are chosen for conducting calculations. DWT decomposes a signal to a set of functions (Cohen and Kovacevic, 1996):

$$\psi_{i,l}(x) = 2^{i/2}\psi_{i,l}^{\left(2^i x - l\right)} \tag{12}$$

where, $\psi_{i,l}(x)$ is generated by another wavelet $\psi(x)$ translated by l and expanded by i. The mother Wavelet should satisfy the following conditions:

$$\int \psi(x)\, dx = 0 \tag{13}$$

The DW function of a signal is computed as follows:

$$c_{i,l} = \int_{-\infty}^{+\infty} f(x)\psi_{i,l}^{*}(x)dx \tag{14}$$

where

$$f(x) = \sum_{i,l} c_{i,l}\, \psi_{i,l}(x)\, dx \tag{15}$$

where, $c_{i,l}$ is the signal estimate coefficient. Form the scaling function ϕ(x), the mother wavelet is presented as:

$$\varphi(x) = \sqrt{2}\sum k_0(n)\varphi(2x-n) \tag{16}$$

$$\psi(x) = \sqrt{2}\sum k_1(n)\varphi(2x-n) \tag{17}$$

where, $k_1 = (-1)^n h_0(1-n)$.

Due to different characteristics of wavelet types, various sets of $k_0(n)$ are considered.

3.2.3. Proposed Wavelet-ELM (WA-ELM)

In this study, time series are divided into several series using the wavelet analysis and then the decomposed components are used as the EM model input. The models provided using WA-ELM are developed through integrating the decomposition ability of series by the wavelet analysis and ELM. In order to employ the wavelet analysis, the MATLAB wavelet toolbox (Misiti et al., 2004) is utilized. The input parameters to the model generated using DWT are in the form of different sub-signals including "A" and "D", where "A" represents the approximation of sub-series and "D" represents details. Fig. 3 illustrates the observed ground water level (GWL) time series of the Baba Nazar well. This time series (S) is decomposed to three-time series (i.e. A1, D1, D2) using the Daubechies mother wavelet with two levels of decomposition. This S series mother wavelet decomposes the measured GWL into an approximation ($A2$) signal and two detailed sub-signals ($D1$, $D2$), so that $S = A2+D1+D2$. The hybrid model proposed in this study (WA-ELM) is shown in Fig. 4.

In order to develop the WA-ELM model, the measured values of the GWL time series in the Baba Nazar station using different mother wavelets and considering two levels are decomposed into different sub-signals including (A(t), D1(t) and D2(t)). By considering different delays, each one of them are decomposed into three sub-series and employed as inputs of the model to determine the model output GWL(t). For modeling WA-ELM, first the mother wavelet and the decomposition level should be identified. Generally, the decomposition level for each specific problem is obtained through the trial and error approach, but recent studies (Nourani et al., 2014) indicate that this level can be calculated as follows:

$$l = \text{int}[\log(n)] \tag{18}$$

where, l is the decomposition level, n is the number of samples and int is the integer part of l. In this study, the value of the data used for training is n = 180, thus the value of the decomposition level is taken into account equal to 2. In fact, in order to model GWL(t) using WL-ELM, despite the number of x delays, the number of model inputs is equal to 3×, so that each of input series are decomposed into three series including A2, D1 and D2. Furthermore, for decomposing the GWL series, five different families including Haar (haar), Daubechies (db), Symlets (sym), Dmeyer (dmey) and Coiflets (coif) are used. In general, by considering different types related to each family, the total number of wavelets types is 24. It is worth noting that the utilization of the wavelet analysis does not necessarily increase the modeling accuracy and the important point is the proper selection of the mother wavelet. In fact, if wavelets are combined well with time series, they increase modeling accuracy. However, the determination of the mother wavelet in such way is not simple and may yield ambiguous results, hence in this study using the trial and error procedure and considering different combinations, the best mother wavelet is detected. In addition, the selection of the input combination taken from different delays has also a significant impact on the results. There is no specific rule for determining effective lags in the GWL estimation, so that most performed studies use the autocorrelation function (ACF) and the partial autocorrelation function (PACF) analysis. However, using of these two analyzes provides no identification of non-linear dependences and choosing effective lag times for time series with the extreme seasonality is not performed well (Barzegar et al., 2017). In this study, the input combinations are selected using the stepwise fitting. In other words, the "stepwisefit" function is used in the MATLAB environment. This function identifies proper parameters for a linear regression. In order to calculate the value of p-value, this function uses the F-test function. The p-value represents the probability of the effect of a specific input in the modeling. The maximum value of p-value is 0.05 and if the value is greater than 0.1, the parameter is eliminated (Silhavy et al., 2017). The input combinations chosen by the stepwise selection are provided as different lags in the form of 10 different models as follows:

Model 1: $\text{GWL}(t) = f(\text{GWL}(t-1))$

Model 2: $\text{GWL}(t) = f(\text{GWL}(t-1), \text{GWL}(t-2))$

Model 3: $\text{GWL}(t) = f(\text{GWL}(t-1), \text{GWL}(t-2), \text{GWL}(t-3))$

Model 4: $\text{GWL}(t) = f(\text{GWL}(t-1), \text{GWL}(t-2), \text{GWL}(t-5))$

Model 5: $\text{GWL}(t) = f(\text{GWL}(t-1), \text{GWL}(t-3), \text{GWL}(t-9))$

Model 6: $\text{GWL}(t) = f(\text{GWL}(t-1), \text{GWL}(t-3), \text{GWL}(t-10))$

Model 7: $\text{GWL}(t) = f(\text{GWL}(t-1), \text{GWL}(t-3), \text{GWL}(t-6))$

Model 8: $\text{GWL}(t) = f(\text{GWL}(t-1), \text{GWL}(t-3), \text{GWL}(t-12))$

Model 9: $\text{GWL}(t) = f(\text{GWL}(t-1), \text{GWL}(t-3), \text{GWL}(t-6), \text{GWL}(t-12))$

Model 10: $\mathrm{GWL}(t) = f(\mathrm{GWL}(t-1), \mathrm{GWL}(t-2), \mathrm{GWL}(t-3), \mathrm{GWL}(t-6), \mathrm{GWL}(t-12))$

4. Results and discussion

4.1. Performance evaluation criteria

In this study, to investigate the accuracy of the numerical models, the statistical indices including the correlation coefficient (*R*), variance account for (*VAF*), Root Mean Squared Error (*RMSE*, Scatter Index (*SI*), Mean Absolute Error (*MAE*), Mean Absolute Percentage Error (*MAPE*), Root Mean Squared Relative Error (*RMSRE*), *BIAS* and Nash–Sutcliffe efficiency coefficient (NSC) are used:

$$R = \frac{\sum_{i=1}^{n}(F_i - \overline{F})(O_i - \overline{O})}{\sqrt{\sum_{i=1}^{n}(F_i - \overline{F})^2 \sum_{i=1}^{n}(O_i - \overline{O})^2}} \tag{19}$$

$$\mathrm{VAF} = \left(1 - \frac{\mathrm{var}(F_i - O_i)}{\mathrm{var}(F_i)}\right) \times 100 \tag{20}$$

$$RMSE = \sqrt{\frac{1}{n}\sum_{i=1}^{n}(F_i - O_i)^2} \tag{21}$$

$$SI = \frac{RMSE}{\overline{O}} \tag{22}$$

$$MAE = \frac{\sum_{i=1}^{n}|F_i - O_i|}{n} \tag{23}$$

$$MAPE = \frac{1}{n}\sum_{i=1}^{n}\left(\frac{|F_i - O_i|}{O_i}\right) \tag{24}$$

$$\mathrm{RMSRE} = \sqrt{\frac{1}{n}\sum_{i=1}^{n}\left(\frac{O_i - F_i}{O_i}\right)^2} \tag{25}$$

$$BIAS = \frac{1}{n}\sum_{i=1}^{n}(F_i - O_i) \tag{26}$$

$$\mathrm{NSC} = 1 - \frac{\sum_{i=1}^{n}(O_i - F_i)^2}{\sum_{i=1}^{n}(O_i - \overline{O})^2} \tag{27}$$

where, O_i is observed values, F_i is simulated values by the numerical models, $\overline{O}$ denotes the average of observed values and n is the number of observed values. First, different activation functions of the ELM model are evaluated and the superior activation function for simulating groundwater level is selected. Preprocessing the raw input variables through the normalization is necessary prior to the calibration of the neural network model (e.g. ELM in this study). Normalization is an extensively used preprocessing technique scaling datasets into an acceptable range. Thus, observed values are normalized and the best normalization coefficients for modeling groundwater level are selected. In the next section, different families of the wavelet model are studied and the superior family is introduced as the mother wavelet. Also in the next sections, ten models of ELM and WA-ELM are investigated and the superior models for each of the ELM and WA-ELM models are chosen. It should be noted that the artificial intelligence models are analyzed in the test mode.

4.2. Evaluation of activation functions

Initially, the activation functions are studied for the ELM model. As discussed, the ELM model has five activation functions including sigmoid, sine, hardlimit, triangle basis and radial basis. In this section, all activation functions are evaluated to identify the superior model. In Table 1, different values of the statistical index for all activation functions of the ELM model are listed. Also, the values of groundwater level simulated by the sigmoid, sine, hardlimit, tribas and radbas activation functions are shown in Fig. 5. For example, the values of *R, RMSE* and *NSC* for the sigmoid activation function are calculated 0.751, 0.954 and 0.333, respectively. Furthermore, the value of *MAE* for this activation function is estimated 0.626. For the sine function, the value of NSC is modeled almost equal to 0.333. However, the sine function simulates the values of *SI* and *BIAS* equal to 0.0006 and −0.216, respectively. It should be noted that the *MAE*, *BIAS* and *NSC* statistical indices for the hardlimit activation function are estimated equal to 1.276, −0.543 and −6.383, respectively. The triangle basis activation function calculates the values of *VAF*, *RMSE* and *NSC* equal to 15.368, 1321 and −0.189, respectively. In addition, the value of the correlation coefficient for the radial basis activation function is equal to 0.651. Also, the values of *MAE*, *MAPE* and *NSC* for this function are calculated 0.990, 0.0005 and −0.189, respectively. As shown, the sigmoid activation function simulates different values of groundwater level with higher accuracy compared to the other activation functions.

4.3. Normalization

As discussed above, the difference between the maximum and minimum groundwater level is very small compared to different values of groundwater, thus Equation (29) is used to normalize different values of groundwater level. Generally, inputting raw data brings about low speed and accuracy of simulation. Input data should be normalized to equalize the value of the data and enhance the speed and accuracy of model. This prevents from excessive decrease of weights. Furthermore, all data are placed between 0 and 1 through normalization. This is beneficial since the output of most of the functions have a threshold between zero and one. In this equation, X represents normalized values, x is the observed value, $x_{\min}$ is the minimum value, $x_{\max}$ is the maximum value and a and b are the normalization coefficients:

$$X = a\left(\frac{x - x_{\min}}{x_{\max} - x_{\min}}\right) + b \tag{28}$$

To normalize the values of x between zero and one, the groundwater

Table 2
Values of statistical indices of a and b normalization coefficients.

Normalization coefficients	*R*	*VAF*	*RMSE*	*SI*	*MAE*	*MAPE*	*RMSRE*	*BIAS*	*NSC*
a = 0.6; b = 0.2	**0.751**	**56.090**	**0.954**	**0.0005**	**0.626**	**0.0003**	**0.0005**	**−0.085**	**0.333**
a = 0.7; b = 0.1	0.691	45.971	1.060	0.0006	0.745	0.0004	0.0006	−0.111	0.203
a = 1; b = 0	0.719	48.952	1.032	0.0006	0.710	0.0004	0.0006	−0.127	0.341
a = 0.8; b = 0	0.726	52.139	0.998	0.0005	0.668	0.0003	0.0005	−0.080	0.260
a = 2; b = −1	0.699	48.084	1.047	0.0006	0.758	0.0004	0.0006	−0.168	0.160

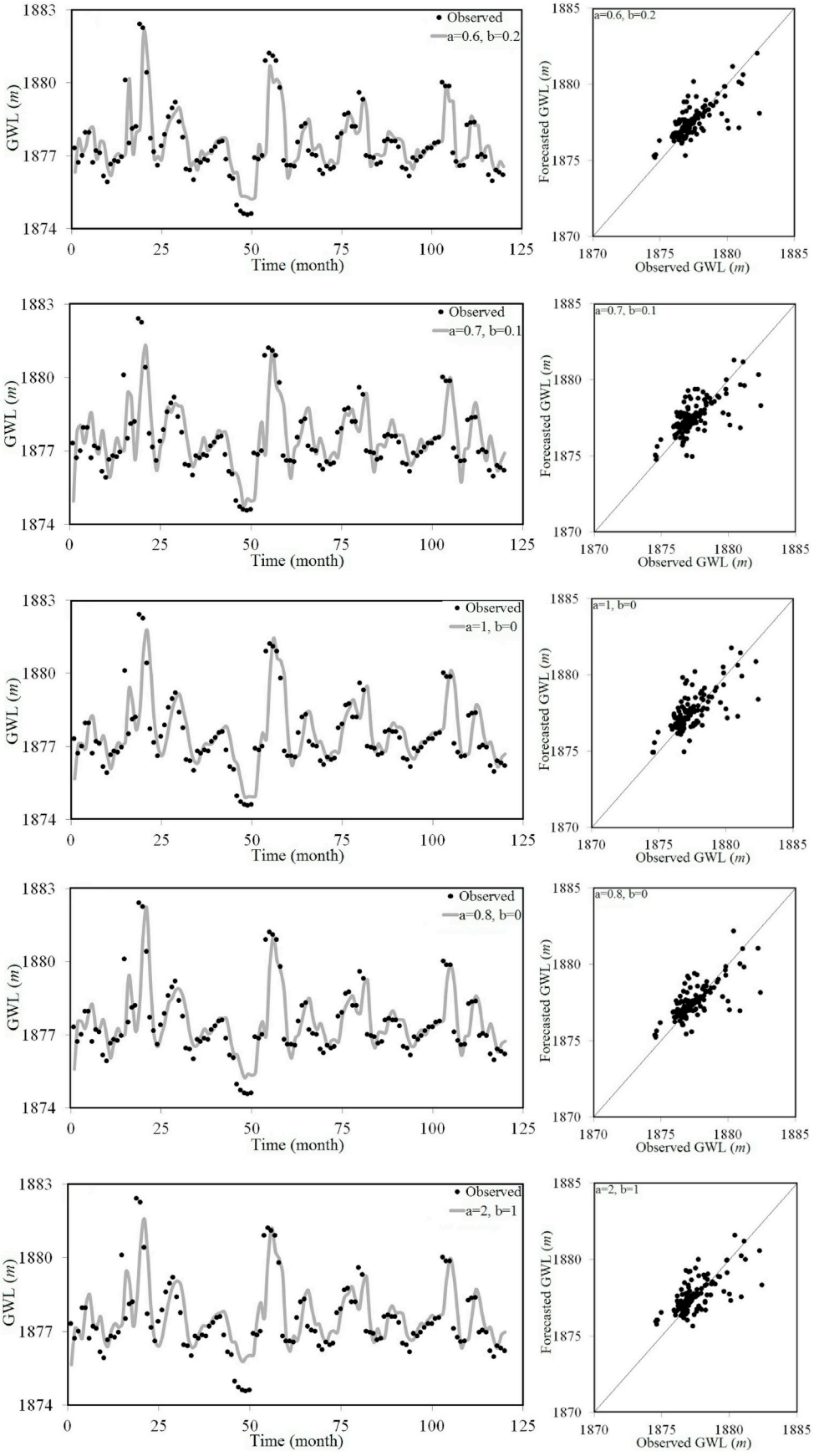

Fig. 6. Modeled groundwater level for models with different normalization coefficients.

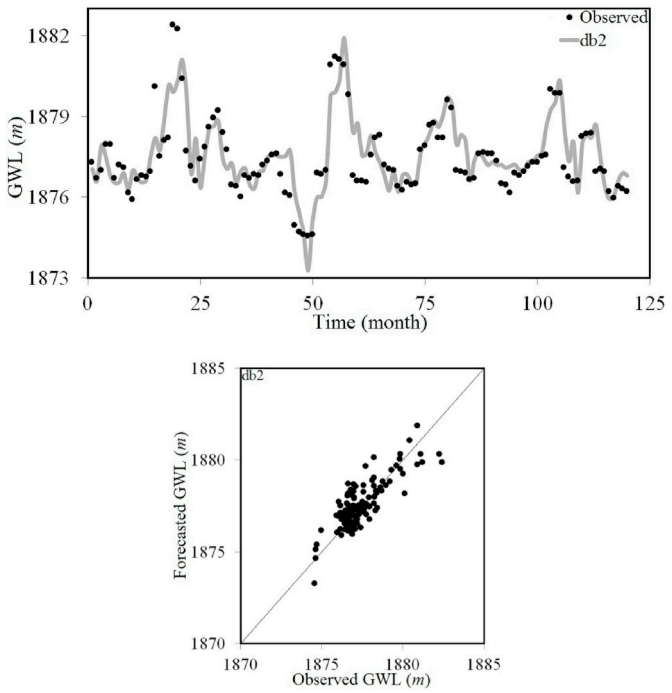

Fig. 7. Modeled groundwater level for selected mother wavelet.

level is simulated for the values of *a* and *b* by the sigmoid activation function selected in the previous section. The results of the statistical indices as well as the simulated groundwater levels are provided in Table 2 and Fig. 6. According to the normalization results, when a = 0.6 and b = 0.2 the values of *R*, *VAF* and *MAE* are estimated equal to 0.751, 56.090 and 0.626, respectively. Also, for these coefficients, the value of the *NSC* index is calculated equal to 0.333, while if a = 0.7 and b = 0.1 the values of *SI*, *BIAS* and *NSC* are estimated equal to 0.0006, −0.111 and 0.203, respectively. Also, the values of the correlation coefficient and the scatter index for the a = 1 and b = 0 normalization coefficients are equal to 0.719 and 0.0006, respectively. For these coefficients, the value of the *NSC* statistical index is also modeled equal to 0.341. In addition, for cases that the normalization coefficients are a = 0.8 and b = 0, the *RMSE* and *MAPE* are calculated equal to 0.998 and 0.0003, respectively. For the a = 2 and b = −1 normalization coefficients, the values of *R*, *MAE* and *NSC* are equal to 0.699, 0.758 and 0.160, respectively. According to the normalization results of groundwater levels, the best a and b coefficients are obtained equal to 0.6 and 0.2, respectively. Additionaly, the simulated groundwater level variations and observed values and the scatter plot for selected mother wavelet is depicted in Fig. 7. Thus, in the next sections, these two coefficients are applied for simulating groundwater level.

4.4. Mother wavelet selection

In this section, the different families of the wavelet model are evaluated. The wavelet model has five different families including haar, db, dmey, sym and coif. The haar family has one member and the db family has ten members, while the dmey, sym and coif families have one, seven and five members, respectively. The results of the calculated statistical indices for different families of the wavelet are listed in Table 3. The analysis of the different families indicates that db2 simulates the values of groundwater level with higher accuracy. For this member of the db family, the values of *R*, *RMSE* and *BIAS* are simulated equal to 0.872, 0.828 and 0.143, respectively. Furthermore, the value of the Nash-Sutcliffe efficiency coefficient for db2 is calculated equal to 0.671. Also, the scatter plot and the simulation results of the groundwater levels for db2 are illustrated in Fig. 2. Thus, db2 is introduced as the mother wavelet in this study.

4.5. Selection of best input combination

In the following, the ELM and WA-ELM models are studied. As discussed, for each of the ELM and WA-ELM models, ten different models are defined. For these models, the superior activation function which is the sigmoid function is selected. Also, the superior normalization coefficients which are a = 0.6 and b = 0.2 are considered for the ELM and WA-ELM models. Also, the number of neurons is started from 2 and continues to 20. The number of neurons increases to some of the extent, however after that this increasing number of neurons does not have a significant impact on modeling accuracy. In this study, for all the ELM and WA-ELM models, the number of neurons is selected equal to 19. Besides for the WA-ELM models, db2 is considered as the mother wavelet. The results of all calculated statistical indices are listed in

Table 3
Values of statistical indices for mother wavelet selection.

Mother wavelet	*R*	*VAF*	*RMSE*	*SI*	*MAE*	*MAPE*	*RMSRE*	*BIAS*	*NSC*
haar	0.350	−254.937	1.371	0.0007	1.012	0.0005	0.0007	0.157	0.097
db1	0.450	−60.048	1.369	0.0007	1.115	0.0006	0.0007	0.242	0.114
db2	**0.827**	**61.236**	**0.828**	**0.0004**	**0.621**	**0.0003**	**0.0004**	**0.143**	**0.671**
db3	0.667	−1.661	1.081	0.0006	0.800	0.0004	0.0006	0.125	0.436
db4	0.652	−29.365	1.097	0.0006	0.809	0.0004	0.0006	0.145	0.421
db5	0.712	23.914	1.070	0.0006	0.858	0.0005	0.0006	0.330	0.471
db6	0.700	21.656	1.048	0.0006	0.797	0.0004	0.0006	0.142	0.471
db7	0.734	27.806	1.055	0.0006	0.868	0.0005	0.0006	0.391	0.496
db8	0.682	−28.696	1.064	0.0006	0.801	0.0004	0.0006	0.169	0.457
db9	0.808	35.666	0.852	0.0005	0.647	0.0003	0.0005	0.055	0.645
db10	0.728	38.176	1.020	0.0005	0.783	0.0004	0.0005	0.112	0.497
dmey	0.720	7.823	1.003	0.0005	0.800	0.0004	0.0005	0.130	0.515
sym2	0.730	20.044	0.991	0.0005	0.771	0.0004	0.0005	0.135	0.527
sym3	0.691	19.388	1.054	0.0006	0.840	0.0004	0.0006	0.041	0.461
sym4	0.761	34.847	0.933	0.0005	0.674	0.0004	0.0005	0.052	0.577
sym5	0.690	11.831	1.069	0.0006	0.829	0.0004	0.0006	0.221	0.458
sym6	0.722	30.713	1.042	0.0006	0.783	0.0004	0.0006	0.264	0.490
sym7	0.600	−16.008	1.170	0.0006	0.901	0.0005	0.0006	0.054	0.336
sym8	0.694	20.800	1.078	0.0006	0.819	0.0004	0.0006	0.246	0.452
coif1	0.695	−8.742	1.036	0.0006	0.784	0.0004	0.0006	0.096	0.481
coif2	0.719	35.817	1.031	0.0005	0.816	0.0004	0.0005	0.082	0.485
coif3	0.693	12.368	1.064	0.0006	0.839	0.0004	0.0006	0.223	0.463
coif4	0.700	7.549	1.037	0.0006	0.824	0.0004	0.0006	0.107	0.480
coif5	0.648	−14.673	1.113	0.0006	0.867	0.0005	0.0006	0.192	0.408

Table 4
Values of statistical indices for different models of ELM and WA-ELM.

Models	*R*	*VAF*	*RMSE*	*SI*	*MAE*	*MAPE*	*RMSRE*	*BIAS*	*Nash*
ELM 1	0.757	37.743	0.948	0.0005	0.611	0.0003	0.0005	0.099	0.565
WA-ELM 1	0.863	66.819	0.726	0.0004	0.528	0.0003	0.0004	0.013	0.743
ELM 2	0.828	60.969	0.824	0.0004	0.569	0.0003	0.0004	0.136	0.672
WA-ELM 2	**0.959**	**91.733**	**0.418**	**0.0002**	**0.344**	**0.0002**	**0.0002**	**0.093**	**0.915**
ELM 3	0.757	33.211	0.946	0.0005	0.626	0.0003	0.0005	0.117	0.568
WA-ELM 3	0.811	57.773	0.857	0.0005	0.622	0.0003	0.0005	0.087	0.644
ELM 4	0.793	53.601	0.916	0.0005	0.617	0.0003	0.0005	0.217	0.602
WA-ELM 4	0.840	63.609	0.789	0.0004	0.532	0.0002	0.0004	0.095	0.699
ELM 5	0.752	31.580	0.958	0.0005	0.667	0.0004	0.0005	0.133	0.558
WA-ELM 5	0.803	55.788	0.877	0.0005	0.607	0.0003	0.0005	0.108	0.629
ELM 6	0.730	−0.626	0.985	0.0005	0.675	0.0004	0.0005	0.073	0.530
WA-ELM 6	0.825	57.710	0.813	0.0004	0.581	0.0003	0.0004	−0.009	0.679
ELM 7	0.768	44.700	0.960	0.0005	0.662	0.0004	0.0005	0.233	0.564
WA-ELM 7	0.887	72.307	0.664	0.0003	0.464	0.0002	0.0003	0.027	0.786
ELM 8	0.768	15.837	0.923	0.0005	0.633	0.0003	0.0005	0.001	0.586
WA-ELM 8	0.856	63.372	0.745	0.0004	0.528	0.0003	0.0004	0.068	0.731
ELM 9	0.761	38.003	0.954	0.0005	0.663	0.0003	0.0005	0.190	0.565
WA-ELM 9	0.848	65.635	0.772	0.0004	0.513	0.0003	0.0004	0.098	0.711
ELM 10	0.817	48.670	0.827	0.0004	0.546	0.0003	0.0004	0.031	0.668
WA-ELM 10	0.855	62.957	0.743	0.0004	0.563	0.0003	0.0004	0.022	0.732

Table 4. According to the modeling results, among all ELM models, ELM 2 simulates the values of groundwater level with higher accuracy compared to the other ELM models. For example, the value of *R* for ELM 2 is calculated equal to 0.828, while the values of *RMSE* and *MAE* for this model are calculated 0.824 and 0.569, respectively. Also, for ELM 2, the values of *BIAS* and Nash are calculated equal to 0.136 and 0.672, respectively. Furthermore, among all the WA-ELM models, the WA-ELM2 model has a higher accuracy compared to the other defined models. In other words, the results of this model have a high correlation with the observed results. For example, the value of the correlation coefficient for WA-ELM 2 is calculated equal to 0.959. Additionally, for this model, the values of the *SI*, *MAE* and *RMSRE* statistical indices are simulated equal to 0.0002, 0.344 and 0.0002, respectively. In addition, for WA-ELM 2, the value of the Nash-Sutcliffe efficiency coefficient is calculated equal to 0.915. In Fig. 8, the scatter plots and the simulation results calculated by the ELM2 and WA-ELM2 models are illustrated. As shown, among all the ELM and WA-ELM models, the WA-ELM 2 model is introduced as the superior model. In the following, the matrix of the WA-ELM 2 model is introduced as follows.

The provided relationship for the WA-ELM2 model with the best performance among all relationships is expressed as follows:

$$GWL\ (t) = \left[\frac{1}{(1 + exp(InW \times InV + BHN))}\right]^{T} \times OutW \tag{29}$$

where, *InV*, *InW*, *OutW* and *BHN* are the matrix of input variables, input weights, output weights and bias of hidden neurons, respectively. The values of this matrix for WA-ELM 2 are presented in the appendix.

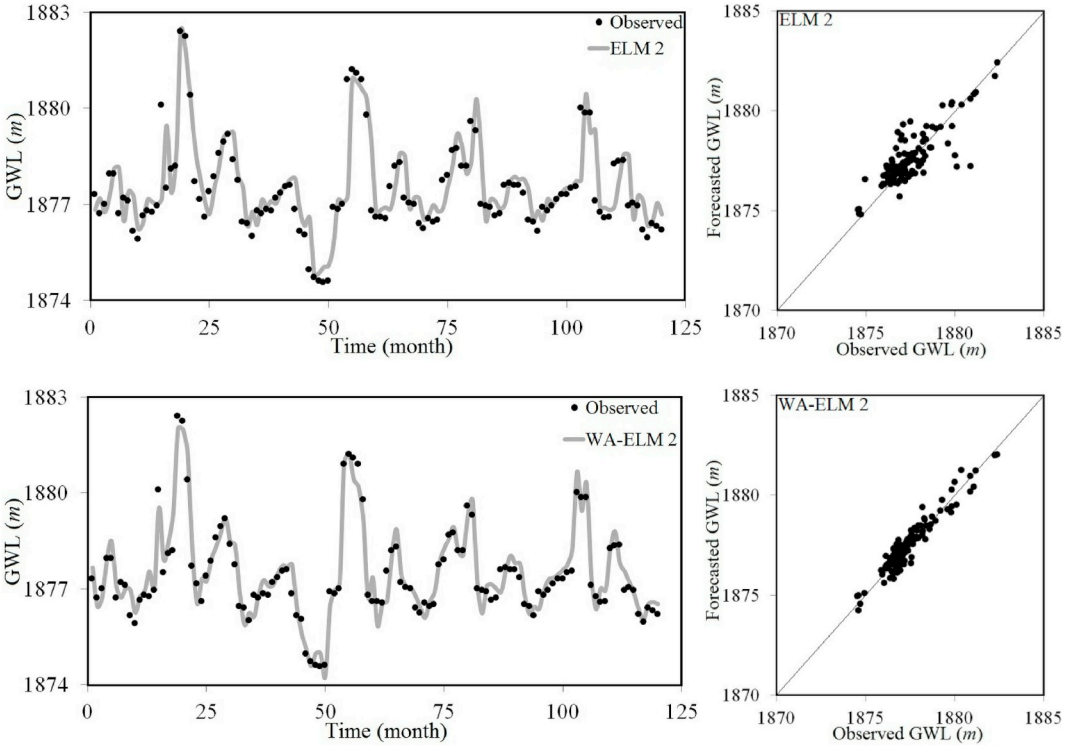

Fig. 8. Modeled groundwater level for superior models of ELM and WA-ELM.

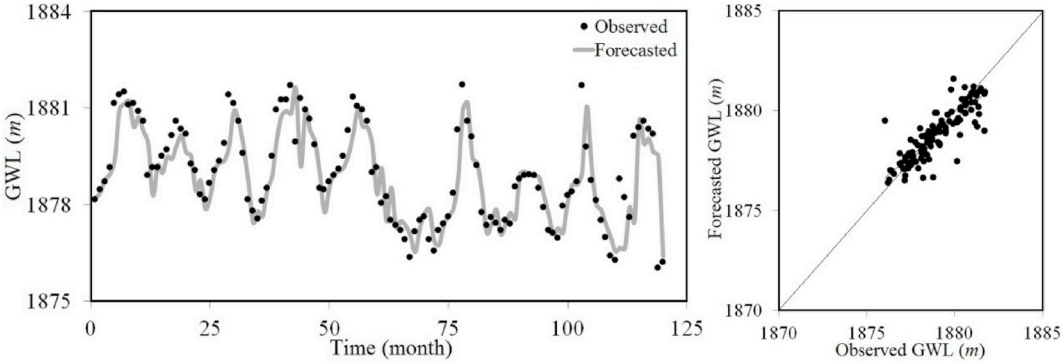

Fig. 9. Comparison of WA-ELM 2 model in simulating groundwater level for the Dastjerd well.

Table 5
Results of different statistical indices for MODFLOW model.

R	VAF	RMSE	SI	MAE	MAPE	RMSRE	BIAS	NSC
0.917	82.677	0.749	0.0004	0.716	0.0004	0.0004	0.030	0.727

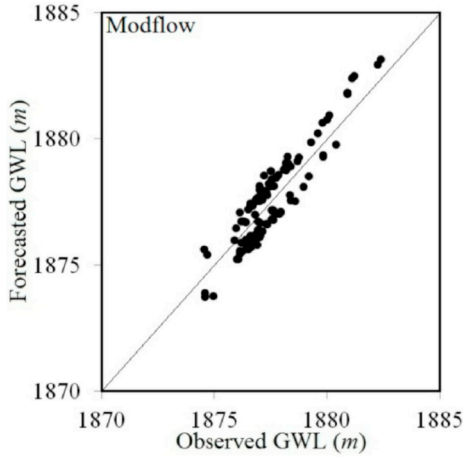

Fig. 10. Scatter plot for groundwater level simulated by MODFLOW.

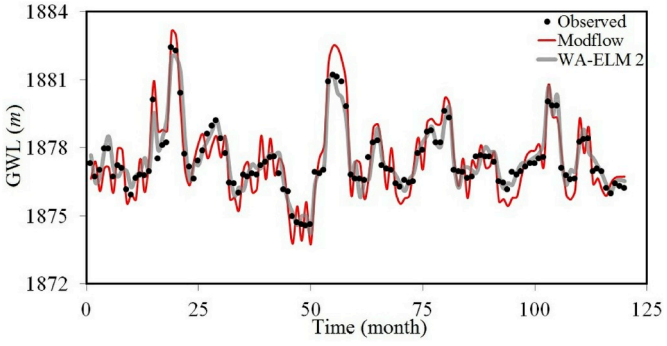

Fig. 11. Comparison of WA-ELM and MODFLOW models in simulating groundwater levelfor Baba Nazar well.

4.6. Verification of WA-ELM 2 model in another piezometer

The accuracy of the superior model (WA-ELM 2) is surveyed for another piezometer (Dastjerd well). The Dastjerd well is located in 35° 14′ 57″ N, 48° 43′ 11″ E. Additionally, the distance between the Baba Nazar and Dastjerd well is about 30 km. In Fig. 9, the scatter plots and the simulated results of the WA-ELM2 model for the Dastjerd well are illustrated. For this well, the correlation coefficient, scatter index and Nash-Sutcliffe efficiency coefficient are calculated 0.851, 0.0004 and 0.862, respectively. Moreover, the RMSE and MAE for this piezometer are estimated 0.796 and 0.542, respectively. As it can be obviously seen, the WA-ELM model has sufficient ability and reasonable accuracy for simulating groundwater level in other piezometers.

Table 6
Uncertainty analysis for ELM 2, WA-ELM 2 and MODFLOW models.

Model	Number of samples	Mean prediction error ($\bar{e}$) (m)	Width of uncertainty band(m)	95% prediction error interval
ELM 2	120	−0.136	−0.024	−0.160 and −0.112
WA-ELM 2	120	−0.093	−0.003	−0.096 and −0.090
MODFLOW	120	−0.030	−0.066	−0.096 and 0.036

4.7. Comparison of WA-ELM and MODFLOW results

In the following, the results of the groundwater level simulated by MODFLOW are studied. In Table 5, the statistical indices calculated for this model are listed. According to the results of the MODFLOW model, the values of the correlation coefficient and the scatter index are modeled equal to 0.917 and 0.0004, respectively. Also, the value of *RMSE* for this model is estimated equal to 0.749. It should be noted that the values of *MAE*, *BIAS* and *NSC* for the MODFLOW model are calculated 0.716, 0.030 and 0.727, respectively. In addition, the scatter plot for the MODFLOW model is shown in Fig. 10.

Furthermore, the results of the superior artificial intelligence (WA-ELM 2) model are compared with the MODFLOW results. The comparison of the WA-ELM 2 and MODFLOW models in simulating the groundwater level for the Baba Nazar well is shown in Fig. 11. According to the modeling results, the WA-ELM 2, simulates the groundwater level values with higher accuracy compared to the MODFLOW model. For example, the value of *R* for the WA-ELM 2 and MODFLOW is modeled equal to 0.959 and 0.917, respectively. Also, for the WA-ELM 2 and MODFLOW models, the value of the Nash-Sutcliffe efficiency coefficient is estimated equal to 0.915 and 0.727, respectively. Furthermore, owing to simple modeling, easy coding and quick computation for simulations in complex yet practical issues, the extreme learning machine (ELM) has recently gained more attention than other models. The ELM models are rarely used probably because they do not significantly improve the accuracy compared to the physically-based models like MODFLOW and/or

engineers are not familiar with the ELM models. To overcome these problems, we develop an ELM model in conjunction with the db2 mother wavelet transform which markedly improves the accuracy of the groundwater simulation.

4.8. Uncertainty analysis

In this section, the uncertainty analysis is conducted for the ELM 2, WA-ELM 2 and MODFLOW models. The uncertainty analysis is used to describe the error obtained by numerical models. The value of the error calculated by numerical models (e_j) is introduced as the difference between computed values (P_j) and observed values (T_j) ($e_j = P_j - T_j$). In contrast, the average of the obtained error is calculated as $\overline{e} = \sum_{j=1}^{n} e_j$, while the value of the standard deviation of calculated error values are defined as $S_e = \sqrt{\sum_{j=1}^{n}(e_j - \overline{e})^2/n-1}$. The negative sign of $\overline{e}$ indicates the underestimated performance of the numerical model. However, the positive sign of $\overline{e}$ indicated the overestimated performance of that model. It should be noted that using the parameters $\overline{e}$ and S_e , a confidence bound is created by the Wilson score method around value predicted from an error without continuity correction. In the following, using $\pm 1.64 S_e$ approximately leads to 95% confidence bound. The uncertainty analysis parameters including the mean prediction error, the width of uncertainty band and the 95% prediction error interval are listed in Table 6 for the ELM 2, WA-ELM 2 and MODFLOW models. For example, the value of $\overline{e}$ for the ELM 2 model is calculated equal to -0.136. Thus, the performance of this model is underestimated. Also, the 95% prediction error interval is estimated between -0.112 and -0.160. Furthermore, the values of $\overline{e}$ for the WA-ELM 2 model are equal to -0.093. Based on the uncertainty analysis results, the WA-ELM 2 model has an underestimated performance. However, the 95% prediction error interval for this model is between -0.090 and -0.096. For the MODFLOW model, the value of the mean prediction error is also calculated as a negative value. Thus, this model has an underestimated performance in estimating groundwater level.

5. Conclusion

One of the most important issues in water resources management is estimating groundwater level. In this paper, the groundwater level in Kabodarahang, Hamadan, Iran was simulated using three models including MODFLOW, Extreme Learning Machine (ELM) and Wavelet-Extreme Learning Machine (WA-ELM). Initially, using the input parameters, ten different models were defined for each of ELM and WA-ELM models. Then, the optimized activation function for the ELM models was chosen. Also, the best mother wavelet was detected for the WA-ELM models. Moreover, the results of the ELM and WA-ELM models were examined and the best soft computing model was introduced. Additionally, the best artificial intelligence model (WA-ELM) was compared with the MODFLOW model. The results of these models showed that the WA-ELM model simulates groundwater level with higher accuracy. For example, for the superior model, the values of *MAE* and *RMSRE* were obtained equal to 0.344 and 0.0002, respectively. In addition, a matrix was provided for the superior model to simulate groundwater level. Furthermore, the uncertainty analysis results showed that the WA-ELM model has an underestimated performance and the 95% prediction error interval for this model was between -0.090 and -0.096.

Appendix. Values of matrix for WA-ELM 2 model

The values of the matrix for WA-ELM 2 are presented as follows:

$$InV = \begin{bmatrix} GWT(t-1)-A2 \\ GWT(t-1)-D1 \\ GWT(t-1)-D2 \\ GWT(t-2)-A2 \\ GWT(t-2)-D1 \\ GWT(t-2)-D2 \end{bmatrix} \tag{30}$$

$$BHN = \begin{bmatrix} 0.57 \\ 0.76 \\ 0.84 \\ 0.95 \\ 0.95 \\ 0.32 \\ 0.12 \\ 0.81 \\ 0.15 \\ 0.98 \\ 0.80 \\ 0.14 \\ 0.12 \\ 0.71 \\ 0.77 \\ 0.40 \\ 0.56 \\ 0.51 \\ 0.93 \end{bmatrix} \quad InW = \begin{bmatrix} -0.64 & -0.11 & -0.36 & 0.10 & -0.02 & 0.54 \\ 0.64 & 0.15 & 0.05 & 0.55 & -0.11 & 0.87 \\ -0.75 & 0.54 & -0.31 & 0.36 & -0.66 & -0.89 \\ 0.32 & 0.11 & -0.73 & 0.84 & 0.11 & -0.08 \\ 0.16 & -0.02 & 0.53 & 0.73 & -0.74 & 0.55 \\ -0.14 & -0.71 & 0.05 & -0.96 & 0.71 & -0.76 \\ -0.18 & 0.64 & -0.23 & -0.38 & -0.87 & -0.72 \\ -0.65 & 0.63 & 0.00 & -0.36 & -0.48 & -0.19 \\ -0.70 & -0.22 & -0.30 & -0.72 & -0.93 & 0.46 \\ 0.12 & -0.20 & 0.80 & -0.37 & -0.50 & -0.07 \\ 0.71 & 0.35 & -0.44 & 0.52 & -0.20 & 0.03 \\ -0.14 & -0.57 & 0.70 & 0.21 & -0.39 & 0.79 \\ 0.18 & -0.43 & -0.52 & -0.72 & 0.19 & 0.77 \\ 0.32 & 0.24 & 0.38 & -0.35 & -0.09 & -0.42 \\ -0.80 & -0.34 & 0.80 & 0.71 & -0.09 & 0.80 \\ -0.79 & -0.64 & -0.28 & -0.50 & 0.23 & 0.27 \\ -0.02 & 0.53 & -0.89 & -0.10 & 0.60 & 0.48 \\ 0.91 & 0.51 & 0.55 & 0.96 & -0.68 & -0.54 \\ 0.17 & 0.03 & 0.87 & -0.69 & 0.42 & -0.93 \end{bmatrix} \quad Outw = \begin{bmatrix} -42732.76 \\ -21.16 \\ 6306.15 \\ 6334.28 \\ -0.02 \\ 6334.82 \\ 6334.82 \\ -1974.44 \\ 7300.87 \\ 69.79 \\ 7300.87 \\ 0.00 \\ 35.88 \\ 542810215.14 \\ 0.00 \\ 7300.87 \\ 0.00 \\ -45238.25 \\ 0.00 \end{bmatrix} \tag{31}$$

References

Barzegar, R., Fijani, E., Moghaddam, A.A., Tziritis, E., 2017. Forecasting of groundwater level fluctuations using ensemble hybrid multi-wavelet neural network-based models. Sci. Total Environ. 599, 20–31.

Bashi-Azghadi, S.N., Kerachian, R., Bazargan-Lari, M.R., Solouki, K., 2010. Characterizing an unknown pollution source in groundwater resources systems using PSVM and PNN. Expert Syst. Appl. 37 (10), 7154–7161.

Boyce, S.E., Nishikawa, T., Yeh, W.W., 2015. Reduced order modeling of the Newton formulation of MODFLOW to solve unconfined groundwater flow. Adv. Water Resour. 83, 250–262.

Chen, M., Izady, A., Abdalla, O.A., 2017. An efficient surrogate-based simulation-optimization method for calibrating a regional MODFLOW model. J. Hydrol. 544, 591–603.

Coelho, C.D., Faria, A.C.S., Marques, E.A.G., 2017. Comparative analysis of different boundary conditions and their influence on numerical hydrogeological modeling of Palmital watershed, southeast Brazil. J. Hydrol.: Reg. Stud. 12, 210–219.

Cohen, A., Kovacevic, J., 1996. Wavelets: the mathematical background. Proc. IEEE 84, 514–522.

Dastorani, M.T., Moghadamnia, A., Piri, J., Rico-Ramirez, M., 2010. Application of ANN and ANFIS models for reconstructing missing flow data. Environ. Monit. Assess. 166 (1–4), 421–434.

Daubechies, I., 1990. The wavelet transform, time–frequency localization and signal analysis. IEEE Trans. Inf. Theory 36 (5).

Dong, Y., Li, G., Xu, H., 2012. An areal recharge and discharge simulating method for MODFLOW. Comput. Geosci. 42, 203–205.

Ebrahimi, H., Rajaee, T., 2017. Simulation of groundwater level variations using wavelet combined with neural network, linear regression and support vector machine. Glob. Planet. Chang. 148, 181–191.

Ghumman, A.R., Ahmad, S., Hashmi, H.N., 2018. Performance assessment of artificial neural networks and support vector regression models for stream flow predictions. Environ. Monit. Assess. 190 (12), 704.

Harbaugh, A.W., Banta, E.R., Hill, M.C., McDonald, M.G., 2000. MODFLOW-2000, the U. S. Geological Survey modular ground-water model-user guide to modularization concepts and the ground-water flow process. Open File Rep. U. S. Geol. Surv. (92), 134.

Heddam, S., Bermad, A., Dechemi, N., 2012. ANFIS-based modelling for coagulant dosage in drinking water treatment plant: a case study. Environ. Monit. Assess. 184 (4), 1953–1971.

Huang, G.B., Zhu, Q.-Y., Siew, C.-K., 2004. Extreme learning machine: a new learning scheme of feedforward neural networks. In: Neural Networks, Proceedings International Joint Conference on, IEEE., vol. 2, pp. 985–990.

Huang, G.B., Chen, L., Siew, C.K., 2006. Universal approximation using incremental constructive feedforward networks with random hidden nodes. IEEE Trans. Neural Netw. 17 (4), 879–892.

Huang, G.B., Chen, L., 2007. Convex incremental extreme learning machine. Neurocomputing 70 (16), 3056–3062.

Huang, G.B., Chen, L., 2008. Enhanced random search based incremental extreme learning machine. Neurocomputing 71 (16), 3460–3468.

Lachaal, F., Mlayah, A., Bédir, M., Tarhouni, J., Leduc, C., 2012. Implementation of a 3-D groundwater flow model in a semi-arid region using MODFLOW and GIS tools: the Zéramdine–BéniHassen Miocene aquifer system (east-central Tunisia). Comput. Geosci. 48, 187–198.

Liu, H., Xie, D., Wu, W., 2008. Soil water content forecasting by ANN and SVM hybrid architecture. Environ. Monit. Assess. 143 (1–3), 187.

Misiti, M., Misiti, Y., Oppenheim, G., Poggi, J.M., 1996. Wavelet Toolbox for Use with Matlab. The Mathworks, Inc., Natick, Massachusetts, USA.

Misiti, M., Misiti, Y., Oppenheim, G., Poggi, J.-M., 2004. Matlab Wavelet Toolbox User's Guide, Version 3.

Nourani, V., Hosseini Baghanam, A., Adamowski, J., Kisi, O., 2014. Applications of hybrid wavelet–Artificial Intelligence models in hydrology: a review. J. Hydrol. 514, 358–377.

Ou, G., Chen, X., Kilic, A., Bartelt-Hunt, S., Li, Y., Samal, A., 2013. Development of a cross-section based streamflow routing package for MODFLOW. Environ. Model. Softw 50, 132–143.

Ou, G., Li, R., Pun, M., Osborn, C., Bradley, J., Schneider, J., Chen, X.H., 2016. A MODFLOW package to linearize stream depletion analysis. J. Hydrol. 532, 9–15.

Silhavy, R., Silhavy, P., Prokopova, Z., 2017. Analysis and selection of a regression model for the use case points method using a stepwise approach. J. Syst. Softw. 125, 1–14.

Update

Groundwater for Sustainable Development
Volume 13, Issue , May 2021, Page

DOI: https://doi.org/10.1016/j.gsd.2021.100594

Groundwater for Sustainable Development 13 (2021) 100594

Contents lists available at ScienceDirect

Groundwater for Sustainable Development

journal homepage: http://www.elsevier.com/locate/gsd

Erratum regarding missing Declaration of Competing Interest statements in previously published articles

Declaration of Competing Interest statements were not included in the published version of the following articles that appeared in previous issues of <<Groundwater for Sustainable Development>>

The appropriate Declaration/Competing Interest statements, provided by the Authors, are included below.

1. "Groundwater potential for irrigation in the Nabogo basin, Northern Region of Ghana" [Groundwater for Sustainable Development, 2019; 9C: 100274] 10.1016/j.gsd.2019.100274

Declaration of competing interest: The Authors have no interests to declare.

2. "Sources of trace elements identification in drinking water of Rangpur district, Bangladesh and their potential health risk following multivariate techniques and Monte-Carlo simulation" [Groundwater for Sustainable Development, 2019; 9C: 100275] 10.1016/j.gsd.2019.100275

Declaration of competing interest: The Authors have no interests to declare.

3. "Assessment of groundwater vulnerability to pollution using two different vulnerability models in Halabja-Saidsadiq Basin, Iraq" [Groundwater for Sustainable Development, 2019; 9C: 100276] 10.1016/j.gsd.2019.100276

Declaration of competing interest: The Authors have no interests to declare.

4. "Preparation of Chitosan-EDTA hydrogel as soil conditioner for soybean plant (Glycine max)" [Groundwater for Sustainable Development, 2019; 9C: 100277] 10.1016/j.gsd.2019.100277

Declaration of competing interest: The Authors have no interests to declare.

5. "Quantitative assessment of water resources by the method of the hydrological balance in the Kadey catchment area (East-Cameroon)" [Groundwater for Sustainable Development, 2019; 9C: 100278] 10.1016/j.gsd.2019.100278

Declaration of competing interest: The Authors have no interests to declare.

6. "Simulation of groundwater level using MODFLOW, extreme learning machine and Wavelet-Extreme Learning Machine models" [Groundwater for Sustainable Development, 2019; 9C: 100279] 10.1016/j.gsd.2019.100279

Declaration of competing interest: The Authors have no interests to declare.

7. "Potential use of UTES in Babylon Governorate, Iraq" [Groundwater for Sustainable Development, 2019; 10C: 100283] 10.1016/j.gsd.2019.100283

Declaration of competing interest: The Authors have no interests to declare.

8. "Performance of MAR model for stormwater management in Barind Tract, Bangladesh" [Groundwater for Sustainable Development, 2019; 10C: 100285] 10.1016/j.gsd.2019.100285

Declaration of competing interest: The Authors have no interests to declare.

9. "A comprehensive assessment of groundwater quality for drinking purpose in a Nigerian rural Niger delta community" [Groundwater for Sustainable Development, 2019; 10C: 100286] 10.1016/j.gsd.2019.100286

Declaration of competing interest: The Authors have no interests to declare.

10. "Simulation performance of single slope solar still by using iteration method for convective heat transfer coefficient." [Groundwater for Sustainable Development, 2019; 10C: 100287] 10.1016/j.gsd.2019.100287

Declaration of competing interest: The Authors have no interests to declare.

11. "Can shallow groundwater sustain small-scale irrigated agriculture in sub-Saharan Africa? Evidence from N-W Ethiopia" [Groundwater for Sustainable Development, 2019; 10C: 100290] 10.1016/j.gsd.2019.100290

Declaration of competing interest: The Authors have no interests to declare.

12. "Groundwater quality assessment using pollution index of groundwater (PIG), ecological risk index (ERI) and hierarchical cluster analysis (HCA): A case study" [Groundwater for Sustainable Development, 2019; 10C: 100292] 10.1016/j.gsd.2019.100292

DOIs of original article: https://doi.org/10.1016/j.gsd.2019.100275, https://doi.org/10.1016/j.gsd.2019.100274, https://doi.org/10.1016/j.gsd.2019.100276, https://doi.org/10.1016/j.gsd.2019.100279, https://doi.org/10.1016/j.gsd.2019.100286, https://doi.org/10.1016/j.gsd.2019.100293, https://doi.org/10.1016/j.gsd.2019.100287, https://doi.org/10.1016/j.gsd.2019.100277, https://doi.org/10.1016/j.gsd.2019.100292, https://doi.org/10.1016/j.gsd.2019.100297, https://doi.org/10.1016/j.gsd.2019.100278, https://doi.org/10.1016/j.gsd.2019.100283, https://doi.org/10.1016/j.gsd.2019.100285, https://doi.org/10.1016/j.gsd.2019.100290, https://doi.org/10.1016/j.gsd.2019.100294.

https://doi.org/10.1016/j.gsd.2021.100594

Available online 19 April 2021

Declaration of competing interest: The Authors have no interests to declare.

13. "Hydrogeochemical studies and suitability assessment of groundwater quality for irrigation at Warri and environs., Niger delta basin, Nigeria" [Groundwater for Sustainable Development, 2019; 10C: 100293] 10.1016/j.gsd.2019.100293

Declaration of competing interest: The Authors have no interests to declare.

14. "A comparison of statistical methods for evaluating missing data of monitoring wells in the Kazeroun Plain, Fars Province, Iran" [Groundwater for Sustainable Development, 2019; 10C: 100294] 10.1016/j.gsd.2019.100294

Declaration of competing interest: The Authors have no interests to declare.

15. "Assessment of ground water quality in Madurai city by using geospatial techniques" [Groundwater for Sustainable Development, 2019; 10C: 100297] 10.1016/j.gsd.2019.100297

Declaration of competing interest: The Authors have no interests to declare.